which reduces the distance between the ruthenium and cobalt centers.[2] The corresponding Os-L-Co series (L = iso(Pro)$_n$) showed a decrease in rate, although lower than expected, in going from n = 2 to n = 3 (Table VI).

The range of rate constants for the Os-L-Co series (factor of 10^7) is much greater than that for the corresponding Ru-L-Co series (factor of 5×10^3) (L = iso(Pro)$_n$, n = 0-4) (Table VI). The effect of distance on the rate is seen more clearly in the Os-L-Co series than in the Ru-L-Co series. This is because in the Os-L-Co series the intramolecular electron-transfer rates depend only on preexisting proline conformers (since the electron-transfer rate is either more rapid or of the same order of magnitude as trans to cis proline isomerization). In contrast, in the Ru-L-Co series the rate can be accelerated by preexisting proline conformers *as well as* conformers formed during the slow electron-transfer process, since the electron-transfer rate is slower than proline isomerization. Therefore, the number of proline conformers which can affect the rate in the Ru-L-Co series is much greater than in the Os-L-Co series.

Based on this analysis, study of even faster electron-transfer systems, where the driving force is increased and/or the reorganization energy of the donor-acceptor set is decreased, should allow further discrimination between the rates for L = iso(Pro)$_n$, n = 2-4. We are currently exploring a series of Os-L-Ru complexes, L = iso(Pro)$_n$, n = 2-4, where such conditions are met.

Acknowledgment. The authors thank Dr. Carol Creutz, Dr. Norman Sutin, and Prof. Henry Taube for helpful discussions. Work done at Rutgers University was supported by the National Institutes of Health Grant GM 26324 and by the National Science Foundation Grant CHE 840552. S.I. is the recipient of a National Institutes of Health Career Development Award (AM 00734) (1980-85) and a Camille and Henry Dreyfus Teacher Scholar Award (1981-85). Work done at Brookhaven National Laboratories is supported by the Office of Basic Energy Science of the Department of Energy.

Registry No. $[(NH_3)_5Co\text{-}i\text{-}Os(NH_3)_5](BF_4)_5$, 98466-52-5; $[(NH_3)_5Co\text{-}(Pro)\text{-}i\text{-}Os(NH_3)_5](BF_4)_5$, 98481-28-8; $[(NH_3)_5Co\text{-}(Pro)_2\text{-}i\text{-}Os(NH_3)_5](BF_4)_5$, 98466-54-7; $[(NH_3)_5Co\text{-}(Pro)_3\text{-}i\text{-}Os(NH_3)_5](BF_4)_5$, 98466-56-9; $[(NH_3)_5Co\text{-}(Pro)_4\text{-}i\text{-}Os(NH_3e_5](BF_4)_5$, 98466-58-1; $[(NH_3)_5Co\text{-}i\text{-}Os(NH_3)_5]^{4+}$, 98466-59-2; $[(NH_3)_5Co\text{-}(Pro)\text{-}i\text{-}Os(NH_3)_5]^{4+}$, 98466-60-5; $[(NH_3)_5\text{-}Co\text{-}(Pro)_2\text{-}i\text{-}Os(NH_3)_5]^{4+}$, 98466-61-6; $[(NH_3)_5Co\text{-}(Pro)_3\text{-}i\text{-}Os(NH_3)_5]^{4+}$, 98466-62-7; $[(NH_3)_5Co\text{-}(Pro)_4\text{-}i\text{-}Os(NH_3)_5]^{4+}$, 98466-63-8; $[(NH_3)_5Co\text{-}(Phe)_2\text{-}i\text{-}Os(NH_3)_5]^{5+}$, 98466-64-9; $[(NH_3)_5Co\text{-}(Gly)_2\text{-}i\text{-}Os(NH_3)_5]^{5+}$, 98466-65-0; $[(NH_3)_5Co\text{-}i\text{-}Ru(NH_3)_4(SO_4)]^{3+}$, 50914-56-2; $[(NH_3)_5Co\text{-}(Pro)\text{-}i\text{-}Ru(NH_3)_4(SO_4)]^{3+}$, 88510-34-3; $[(NH_3)_5Co\text{-}(Pro)_2\text{-}i\text{-}Ru(NH_3)_4(SO_4)]^{3+}$, 88524-97-4; $[(NH_3)_5Co\text{-}(Pro_3)\text{-}i\text{-}Ru(NH_3)_4(SO_4)]^{3+}$, 88525-00-2; $[(NH_3)_5Co\text{-}(Pro)_4\text{-}i\text{-}Ru(NH_3)_4(SO_4)]^{3+}$, 88525-03-5.

Edge-Sharing Bioctahedral Dimolybdenum(III) Molecules with μ-RS Groups. Direct Experimental Evidence for Spin-State Equilibria

F. Albert Cotton,*[1a] Michael P. Diebold,[1a] Charles J. O'Connor,[1b] and Gregory L. Powell[1a]

Contribution from Department of Chemistry and Laboratory for Molecular Structure and Bonding, Texas A&M University, College Station, Texas 77843, and Department of Chemistry, University of New Orleans Lakefront, New Orleans, Louisiana 70148. *Received June 5, 1985*

Abstract: A series of dimolybdenum(III) molecules with edge-sharing bioctahedral structures and general formula (LL)$MoCl_2(\mu\text{-}SR)_2MoCl_2$(LL) have been prepared: namely—**1**, LL = dto, R = Et; **2**, LL = dmpe, R = Et; **3**, LL = dtd, R = Et; **4**, LL = dto, R = Ph; **5**, LL = dmpe, R = Ph; **6**, LL = dtd, R = Ph (dto = $EtSCH_2CH_2SEt$; dtd = $PrSCH_2CH_2SPr$; dmpe = $Me_2PCH_2CH_2PMe_2$). Principal methods of preparation are (a) $Mo_2Cl_8^{4-}$ + 2LL + RSSR and (b) $Mo_2Cl_4(LL)_2$ + RSSR. Compounds **1** and **2** have been structurally characterized by X-ray crystallography. In each case there is a central, planar (LL)$Mo(\mu\text{-}SR)_2Mo$(LL) unit with chlorine atoms above and below this plane on each molybdenum atom. Compound **1** forms crystals in space group $C2/c$ with a = 18.114 (4) Å, b = 9.925 (1) Å, c = 16.403 (4) Å, β = 97.76 (2)°, Z = 4. The Mo-Mo distance is 2.682 (1) Å. Compound **2** forms crystals in space group $Pnmn$ with a = 12.835 (3) Å, b = 15.705 (5) Å, c = 9.046 (2) Å, Z = 2. The Mo-Mo distance is 2.712 (3) Å. Compounds **1**, **2**, and **4** have been characterized magnetically and exhibit temperature-dependent magnetic properties consistent with the thermal population of an excited triplet state based on the $\delta^*\delta$ configuration.

Complexes containing two metal atoms that are held in proximity within a set of ten ligand atoms defining an edge-sharing bioctahedron afford an opportunity to study metal-metal interactions as many ligand properties are varied. The situation is attractive because of the practical possibilities that exist for systematically controlling and manipulating the circumstances in which these interactions occur, provided of course that synthetic methods can be devised to generate the desired sets of ligands surrounding a given pair of metal ions. This type of structural situation is deserving of study because it is found very commonly in coordination chemistry and solid-state chemistry.

In these laboratories we are engaged in developing synthetic methods that will provide designed access to new M_2L_{10} species and also in carrying out the structural, spectroscopic, magnetic, and theoretical studies necessary to develop an understanding of the consequent M-M interactions. In this paper we report in detail on the preparation and characterization of dimolybdenum(III) compounds containing bridging RS^- groups (R = Et, Ph). Not only are these the first such compounds to be reported, but the synthetic method, viz., oxidative addition to Mo-Mo quadruple bonds, is both novel and capable of being generalized. We also give detailed experimental results and analysis of the magnetic properties of three of these complexes. Portions of this work have been previously published in a preliminary communication.[2]

(1) Texas A&M University. (b) University of New Orleans.

0002-7863/85/1507-7438$01.50/0

Experimental Section

Diphenyl disulfide (PhSSPh) was purchased from Aldrich Chemical Co., 3,6-dithiaoctane (dto) and diethyl disulfide (EtSSEt) from Pfaltz and Bauer, Inc., and 4,7-dithiadecane (dtd) from ICN Pharmaceutical, Inc. All preparations were carried out under dry, air-free atmospheres with carefully dried, deoxygenated solvents. Infrared spectra were recorded with a Perkin-Elmer 783 spectrophotometer on mineral oil mull samples.

Preparation of $Mo_2(\mu\text{-SEt})_2Cl_4(dto)_2$ (1). A. Reaction of $Mo_2Cl_8^{4-}$ with dto. A mixture of $K_4Mo_2Cl_8$ (0.51 g, 0.81 mmol), dto (0.60 mL, 3.9 mmol), and methanol (30 mL) was refluxed for 2 days and then allowed to slowly cool to room temperature. After 4 more days, the mixture was filtered in air on a medium glass frit. Along with some KCl and some unreacted $K_4Mo_2Cl_8$, several large, green crystals of **1** were separated from the brown filtrate. The green product was isolated in pure form by washing the solids with water (40 mL) and ethanol (20 mL). Yield: 0.073 g (12%).

B. Reaction of $Mo_2Cl_8^{4-}$ with EtSSEt and dto. Ethyl disulfide (EtSSEt) (0.41 mL, 3.3 mmol) was added to a flask containing 1.94 g (3.13 mmol) of $(NH_4)_5Mo_2Cl_9\cdot H_2O$ and 80 mL of methanol. Immediately, 1.0 mL (6.5 mmol) of dto was also added. The mixture was stirred and refluxed for 5 h to yield a red-brown solution and a yellow-green precipitate. The solid was filtered off, washed with 15 mL of ethanol, and dried in vacuo. An IR spectrum of this product was identical with that of the product isolated in reaction A above. Yield: 0.327 g (14%). In addition, the filtrate was pumped to dryness and the residue found to be a mixture of **1** and a brown solid which will be referred to as **1a**. Other than the measurement of its IR spectrum, no effort was made to characterize this brown product.

This same procedure was repeated with half the original volume of methanol and including a boiling stick. Compound **1** was isolated in 49% yield as dark green crystals adhering to the boiling stick. The identity of these crystals was confirmed by both IR spectroscopy and X-ray crystallography (the unit cell parameters were essentially the same as those for the crystals produced in reaction A).

With use of the same amounts of reactants as first described above, this procedure was repeated once more except that the EtSSEt and $Mo_2Cl_8^{4-}$ were allowed to reflux together for 1 h before the addition of dto. No trace of $Mo_2(\mu\text{-SEt})_2Cl_4(dto)_2$ was obtained. Instead, **1a** precipitated from a red-brown solution.

C. Reaction of $Mo_2Cl_4(dto)_2$ with EtSSEt. A mixture of 0.50 g (0.79 mmol) of $Mo_2Cl_4(dto)_2$,[3-5] 0.10 mL (0.81 mmol) of EtSSEt, and 40 mL of methanol was refluxed for 2 h to give a brown solution and a green-brown precipitate. This mixture was filtered, and the volume of the filtrate was reduced by vacuum to ca. 5 mL, yielding more green-brown solid. The solids were washed with water (20 mL) and ethanol (5 mL) and dried in vacuo. The product was identified as compound **1** by comparison of its IR spectrum with that of the product from procedure A. Yield: 0.49 g (82%).

Preparation of $Mo_2(\mu\text{-SEt})_2Cl_4(dmpe)_2\cdot C_7H_8$ (2). β-$Mo_2Cl_4(dmpe)_2$[6] (0.37 g, 0.58 mmol) and EtSSEt (0.09 mL, 0.69 mmol) were stirred together in 25 mL of toluene at 65 °C for 16 h to produce a red-brown solution with a small amount of brown solid. The volume of the solution was reduced to ca. 5 mL by vacuum distillation, and 30 mL of hexane was added to precipitate more product. After this mixture was stirred for 1 h and then cooled at 5 °C for 5 h, the solid product was filtered off in air and washed with hexane (20 mL). Yield: 0.35 g (80%).

In order to obtain crystals suitable for X-ray crystallographic study, the above procedure was repeated with the following modifications. After the period of heating and stirring, the volume of the reaction solution was reduced under vacuum to ca. 15 mL. Hexane was then added until the solution became slightly cloudy. This mixture was then cooled at −20 °C to yield several small, single crystals.

Preparation of $Mo_2(\mu\text{-SEt})_2Cl_4(dtd)_2$ (3). A solution of 1.0 mL of EtSSEt in 50 mL of methanol was prepared and 0.78 mL of this solution (ca. 0.124 mmol of EtSSEt) was added to a solution of 0.085 g (0.123 mmol) of $Mo_2Cl_4(dtd)_2$[5] in 15 mL of chloroform. A red-brown solution and a brown precipitate resulted after 9 h of stirring and refluxing. This mixture was pumped to dryness under vacuum and the residue extracted with a minimal amount of warm methanol. After being cooled at −20 °C for 3 days, the product was filtered off and dried in vacuo. Yield: 0.075 g (75%).

Preparation of $Mo_2(\mu\text{-SPh})_2Cl_4(dto)_2$ (4). A. Reaction of $Mo_2Cl_8^{4-}$ with PhSSPh and dto. A mixture of 0.901 g (1.42 mmol) of $K_4Mo_2Cl_8$, 0.320 g (1.47 mmol) of diphenyl disulfide (PhSSPh), and 0.5 mL (3.2 mmol) of dto in 80 mL of methanol was refluxed for 2 days and then cooled at 5 °C for 1 day. The resulting mixture was filtered to separate a yellow-green precipitate from a brown solution. The filtrate was pumped to dryness under vacuum and the residue extracted with 35 mL of CH_2Cl_2. After the mixture was cooled at −10 °C for several days, filtration gave more yellow-green product. The combined precipitates of **4** were washed with 50 mL of water and 30 mL of hexane and then dried in vacuo. Yield: 0.39 g (32%). The second filtrate was again pumped to dryness and a brown solid was scraped from the flask and washed with toluene and hexane. An IR spectrum of this brown product was different from that of **4** but similar to that of **1a**. It will be referred to as **4a**.

B. Reaction of $Mo_2Cl_4(dto)_2$ with PhSSPh. $Mo_2Cl_4(dto)_2$ (0.15 g, 0.24 mmol) and PhSSPh (0.06 g, 0.27 mmol) were stirred and refluxed together in 15 mL of methanol for 1.5 h to produce a brown solution and a yellow-green solid. The volume of the solution was reduced to ca. 4 mL by evaporation under a stream of nitrogen. The yellow-green product was filtered off, washed with hexane, and dried in vacuo. An IR spectrum of this compound was identical with that of the product from reaction A. Yield: 0.16 g (79%).

Preparation of $Mo_2(\mu\text{-SPh})_2Cl_4(dmpe)_2$ (5). β-$Mo_2Cl_4(dmpe)_2$[6] (0.27 g, 0.43 mmol) and PhSSPh (0.11 g, 0.50 mmol) were stirred and refluxed together in 30 mL toluene for 3 h to give a brown solution and a brown precipitate. The volume of the solution was reduced to ca. 3 mL by evaporation under N_2, and the brown product was filtered off and washed with hexane. Yield: 0.32 g (87%).

Preparation of $Mo_2(\mu\text{-SPh})_2Cl_4(dtd)_2$ (6). A mixture of 0.29 g (0.42 mmol) of $Mo_2Cl_4(dtd)_2$, 0.10 g (0.46 mmol) of PhSSPh, and 25 mL of CH_2Cl_2 was refluxed for 18 h. After the volume was reduced to 5 mL by evaporation, the brown product was filtered from a brown solution and washed with hexane. Yield: 0.27 g (71%).

Reaction of $Mo_2Cl_4(dppm)_2$ with PhSSPh. $Mo_2Cl_4(dppm)_2\cdot 2THF$[7] (0.60 g, 0.51 mmol) and PhSSPh (0.12 g, 0.55 mmol) were refluxed in 30 mL of CH_2Cl_2 for 13 h. The resulting green solution was cooled at −20 °C for 3 days. Green crystals of $Mo_2Cl_4(dppm)_2$ were recovered in 88% yield, thus no reaction had occurred.

Reaction of $Mo_2Cl_4(PMe_3)_4$ with EtSSEt. A mixture of 0.64 g (1.0 mmol) of $Mo_2Cl_4(PMe_3)_4$,[8] 0.13 mL (1.1 mmol) of EtSSEt, and 20 mL of toluene was refluxed for 12 h with no change in appearance. Cooling at −20 °C for several days afforded crystals of $Mo_2Cl_4(PMe_3)_4$. After these crystals were filtered off, hexane was added to the filtrate to precipitate more starting material. The total amount of $Mo_2Cl_4(PMe_3)_4$ recovered was 0.62 g (97%).

Reaction of $Mo_2Cl_4(PMe_2Ph)_4$ with EtSSEt. A mixture of 0.873 g (0.985 mmol) of $Mo_2Cl_4(PMe_2Ph)_4$,[9] 0.14 mL (1.1 mmol) of EtSSEt, and 22 mL of toluene was refluxed for 15 h. $Mo_2Cl_4(PMe_2Ph)_4$ (0.83 g, 95%) was recovered by adding hexane to the "reaction" mixture and filtering the mixture through a medium frit and washing it with more hexane.

X-ray Crystallography. The structures of compounds **1** and **2** were determined, by employing methods that have been previously described.[10-12] Details specific to these two compounds are summarized in Table I. In neither case was there any indication of crystal decay during data collection. Empirical absorption corrections, which were small, were made based on azimuthal (ψ) scans of reflections with Eulerian angle χ near 90°.

(2) Cotton, F. A.; Powell, G. L. *J. Am. Chem. Soc.* **1984**, *106*, 3371.
(3) This compound, reported previously,[4] was prepared according to a general procedure for other such $Mo_2Cl_4(LL)_2$ compounds with LL = $RSCH_2CH_2SR$ by San Filippo et al.[5]
(4) Cotton, F. A.; Fanwick, P. E.; Fitch, J. W., III *Inorg. Chem.* **1978**, *17*, 3254.
(5) San Filippo, J., Jr.; Sniadoch, H. J.; Grayson, R. L. *Inorg. Chem.* **1974**, *13*, 2121.
(6) Cotton, F. A.; Powell, G. L. *Inorg. Chem.* **1983**, *22*, 1507.
(7) Green, M. L. H.; Parkin, G.; Bashkin, J.; Fail, J.; Prout, K. *J. Chem. Soc., Dalton Trans.* **1982**, 2519.
(8) Cotton, F. A.; Extine, M. W.; Felthouse, T. R.; Kolthammer, B. W. S.; Lay, D. G. *J. Am. Chem. Soc.* **1981**, *103*, 4040.
(9) San Filippo, J. *Inorg. Chem.* **1972**, *11*, 3140.
(10) (a) Bino, A.; Cotton, F. A.; Fanwick, P. E. *Inorg. Chem.* **1979**, *18*, 3558. (b) Cotton, F. A.; Frenz, B. A.; Deganello, G.; Shaver, A. *J. Organomet. Chem.* **1973**, *50*, 227.
(11) North, A. C. T.; Phillips, D. C.; Mathews, F. S. *Acta Crystallogr., Sect. A* **1968**, *24*, 351.
(12) Crystallographic calculations were done with either Enraf–Nonius SDP software on a PDP-11/60 computer at B. A. Frenz & Assoc., College Station, TX, or VAXSDP software on the VAX-11/780 computer at the Department of Chemistry, Texas A&M University.
(13) Agaskar, P. A.; Cotton, F. A.; Derringer, D. R.; Powell, G. L.; Root, D. R.; Smith, T. J. *Inorg. Chem.* **1985**, *24*, 2786.
(14) Chakravarty, A. R.; Cotton, F. A.; Diebold, M. P.; Lewis, D. B.; Roth, W. J. *J. Am. Chem. Soc.*, in press.
(15) Sattelberger, A. P.; Wilson, R. B., Jr.; Huffman, J. C. *Inorg. Chem.* **1982**, *21*, 2392.

Table I. Summary of X-ray Crystallographic Parameters for Compounds **1** and **2**

compound	$Mo_2(\mu\text{-}SEt)_2Cl_4(dto)_2$ (**1**)	$Mo_2(\mu\text{-}SEt)_2Cl_4(dmpe)_2\cdot C_7H_8$ (**2**)
formula	$Mo_2Cl_4S_6C_{16}H_{38}$	$Mo_2Cl_4S_2P_4C_{23}H_{50}$
formula wt	756.53	848.36
space group	$C2/c$	$Pnmn$
a, Å	18.114 (4)	12.835 (3)
b, Å	9.925 (1)	15.705 (5)
c, Å	16.403 (4)	9.046 (2)
α, deg	90	90
β, deg	97.76 (2)	90
γ, deg	90	90
V, Å^3	2922 (2)	1823 (1)
Z	4	2
d_{calcd}, g/cm^3	1.720	1.545
crystal size, nm	0.28 × 0.30 × 0.50	0.10 × 0.14 × 0.25
μ(Mo Kα), cm^{-1}	16.27	12.65
data collection instrument	CAD-4	Syntex P$\bar{1}$
scan method	ω–2θ	ω–2θ
data collection range (2θ)	5–50°	5–50°
no. of unique data, total with $F_o^2 > 3\sigma(F_o^2)$	2192	633
no. of parameters refined	127	77
R^a	0.0307	0.0464
$R_w{}^b$	0.0589	0.0608
quality of fit indicator^c	1.960	1.264
largest shift/esd, final cycle	0.03	0.19
largest peak (e/Å^3) in final diff map	0.77	1.05

$^a R = \sum||F_o| - |F_c||/\sum|F_o|$. $^b R_w = [\sum w(|F_o| - |F_c|)^2/\sum w|F_o|^2]^{1/2}$; $w = 1/\sigma(|F_o|^2)$. ^{c}Quality of fit = $[\sum w(|F_o| - |F_c|)^2/(N_{obsd} - N_{parameters})]^{1/2}$.

Table II. Positional and Isotropic Equivalent Thermal Parameters for $Mo_2(\mu\text{-}SEt)_2Cl_4(dto)_2$ (**1**)[a,b]

atom	x	y	z	B (Å^2)
Mo	0.23280 (2)	0.13589 (4)	−0.04209 (2)	2.057 (7)
Cl(1)	0.19507 (7)	0.0034 (1)	0.06768 (7)	3.09 (2)
Cl(2)	0.26360 (7)	0.2069 (1)	−0.17346 (7)	3.25 (2)
S(1)	0.14430 (6)	0.3098 (1)	−0.02357 (7)	2.62 (2)
S(2)	0.29219 (7)	−0.0928 (1)	−0.06994 (7)	2.57 (2)
S(3)	0.12201 (7)	0.0381 (1)	−0.13934 (7)	2.80 (2)
C(1)	0.1205 (3)	0.4022 (6)	−0.1214 (4)	4.4 (1)
C(2)	0.0695 (4)	0.5207 (6)	−0.1104 (4)	5.4 (2)
C(11)	0.1633 (3)	−0.1033 (5)	−0.1864 (3)	2.9 (1)
C(12)	0.0550 (3)	−0.0405 (6)	−0.0799 (3)	4.0 (1)
C(13)	−0.0122 (3)	−0.1009 (8)	−0.1364 (4)	5.1 (1)
C(21)	0.2158 (3)	−0.1879 (5)	−0.1227 (3)	3.0 (1)
C(22)	0.3548 (3)	−0.0823 (6)	−0.1488 (3)	3.6 (1)
C(23)	0.4020 (3)	−0.2096 (6)	−0.1494 (4)	4.5 (1)

[a] Anisotropically refined atoms are given in the form of the isotropic equivalent thermal parameter defined as the following: $^4/_3[a^2\beta_{11} + b^2\beta_{22} + c^2\beta_{33} + ab(\cos\gamma)\beta_{12} + ac(\cos\beta)\beta_{13} + bc(\cos\alpha)\beta_{23}]$. [b] Estimated standard deviations in the least significant digits are given in parentheses.

Table III. Bond Distances (Å) and Angles (deg) for $Mo_2(\mu\text{-}SEt)_2Cl_4(dto)_2$ (**1**)

Distances			
Mo–Mo′	2.682 (1)	S(2)–C(21)	1.798 (4)
Mo–Cl(1)	2.402 (1)	S(2)–C(22)	1.835 (4)
Mo–Cl(2)	2.403 (1)	S(3)–C(11)	1.811 (4)
Mo–S(1)	2.403 (1)	S(3)–C(12)	1.831 (4)
Mo–S(1)′	2.400 (1)	C(1)–C(2)	1.522 (6)
Mo–S(2)	2.579 (1)	C(11)–C(21)	1.559 (5)
Mo–S(3)	2.579 (1)	C(12)–C(13)	1.548 (6)
S(1)–C(1)	1.848 (4)	C(22)–C(23)	1.526 (6)
Angles			
Mo′–Mo–Cl(1)	98.42 (3)	S(1)′–Mo–S(2)	83.87 (3)
Mo′–Mo–Cl(2)	98.51 (3)	S(1)′–Mo–S(3)	163.63 (3)
Mo′–Mo–S(1)	55.99 (2)	S(2)–Mo–S(3)	82.39 (3)
Mo′–Mo–S(1)′	56.11 (2)	Mo–S(1)–Mo′	67.90 (3)
Mo′–Mo–S(2)	139.56 (3)	Mo–S(1)–C(1)	109.1 (2)
Mo′–Mo–S(3)	138.05 (3)	Mo–S(1)′–C(1)′	111.8 (2)
Cl(1)–Mo–Cl(2)	163.04 (3)	Mo–S(2)–C(21)	103.6 (1)
Cl(1)–Mo–S(1)	92.09 (3)	Mo–S(2)–C(22)	112.8 (2)
Cl(1)–Mo–S(1)′	97.31 (3)	C(21)–S(2)–C(22)	101.5 (2)
Cl(1)–Mo–S(2)	79.55 (3)	Mo–S(3)–C(11)	102.9 (1)
Cl(1)–Mo–S(3)	88.91 (3)	Mo–S(3)–C(12)	110.3 (1)
Cl(2)–Mo–S(1)	98.18 (3)	C(11)–S(3)–C(12)	103.8 (2)
Cl(2)–Mo–S(1)′	91.32 (3)	S(1)–C(1)–C(2)	110.8 (3)
Cl(2)–Mo–S(2)	86.92 (3)	S(3)–C(11)–C(21)	112.4 (2)
Cl(2)–Mo–S(3)	79.12 (3)	S(3)–C(12)–C(13)	111.7 (3)
S(1)–Mo–S(1)′	112.10 (3)	S(2)–C(21)–C(11)	113.5 (3)
S(1)–Mo–S(2)	162.96 (3)	S(2)–C(22)–C(23)	110.9 (3)
S(1)–Mo–S(3)	82.64 (3)		

Compound **1** was treated from the outset in space group $C2/c$, and this was confirmed (as compared to Cc) by successful refinement. The Mo position was determined from a Patterson map, and the other non-hydrogen atoms were located through alternating series of least-squares refinements and difference Fourier maps. All atoms were refined anisotropically. Final atomic positional and isotropic-equivalent thermal parameters are listed in Table II. Anisotropic thermal parameters are available as supplementary material and bond distances and angles are given in Table III.

For compound **2**, axial photographs revealed the crystal system as orthorhombic and systematic absences indicated two possible space groups, $Pn2n$ and $Pnmn$. The structure was successfully refined in $Pnmn$ (a nonstandard setting of $Pnnm$). The location of the Mo atom was determined from a Patterson map, and all other non-hydrogen atoms were located through a series of least-square refinements and difference Fourier maps.

After complete anisotropic refinement of the principal molecule, a difference map contained three peaks indicative of a distorted six-membered ring. These peaks were refined as carbon atoms and assumed to correspond to a toluene molecule. The presence of toluene of solvation was confirmed by an IR spectrum of the crystals. The three carbon

(16) To a first-order approximation, the metal ion d orbitals of octahedral e_g symmetry are involved in the metal-to-ligand bonding. The remaining t_{2g} set of d orbitals that contain the unpaired electrons of the Mo(III) ion are involved in metal–metal bonding. The metal ion orbitals that are to participate in metal–metal bonding for complexes of D_{2h} symmetry may be defined in terms of the d-orbital basis set as follows:

$$d_\sigma = d_{xy}$$

$$d_\pi = 2^{1/2}(d_{xz} + d_{yz})$$

$$d_\delta = 2^{1/2}(d_{xz} - d_{yz})$$

These atomic orbitals on the two ion centers then overlap as indicated in Figure 5.

(17) Shaik, S.; Hoffmann, R.; Fisel, C. R.; Summerville, R. H. *J. Am. Chem. Soc.* **1980**, *102*, 4555.
(18) Cotton, F. A.; Fang, A. *J. Am. Chem. Soc.* **1982**, *104*, 113.
(19) Cotton, F. A.; Diebold, M. P.; Shim, I. *Inorg. Chem.* **1985**, *24*, 1510.
(20) Hall, M. B.; Fenske, R. F. *Inorg. Chem.* **1972**, *11*, 768.
(21) Anderson, L. B.; Cotton, F. A.; DeMarco, D.; Fang, A.; Ilsley, W. H.; Kolthammer, B. W. S.; Walton, R. A. *J. Am. Chem. Soc.* **1981**, *103*, 5078.
(22) Cotton, F. A.; Roth, W. J. *Inorg. Chem.* **1983**, *22*, 3654.
(23) Cotton, F. A.; Roth, W. J.; *Inorg. Chim. Acta* **1983**, *71*, 175.
(24) Boorman, P. M.; Ball, J. M.; Moynihan, K. J.; Patel, V. D.; Richardson, J. F. *Can. J. Chem.* **1984**, *61*, 2809.

Table IV. Positional and Isotropic Equivalent Thermal Parameters for $Mo_2(\mu\text{-}SEt)_2Cl_4(dmpe)_2\cdot C_7H_8$ (**2**)[a,b]

atom	*x*	*y*	*z*	*B* (Å^2)
Mo	0.0	0.08635 (9)	0.0	2.31 (2)
Cl	0.1331 (3)	0.1092 (2)	−0.1847 (4)	3.76 (7)
P	−0.0928 (3)	0.2107 (2)	−0.1222 (4)	4.10 (9)
S	0.1160 (4)	0.0	0.1465 (5)	3.1 (1)
C(1)	0.080 (2)	0.0	0.345 (2)	3.8 (5)
C(2)	0.183 (2)	0.0	0.439 (3)	7.3 (7)
C(3)	−0.059 (1)	0.3098 (8)	−0.018 (2)	6.1 (4)
C(4)	−0.237 (1)	0.209 (1)	−0.125 (2)	7.3 (5)
C(5)	−0.058 (1)	0.240 (1)	−0.309 (2)	6.1 (4)
C(A)	0.079 (2)	0.5	0.5	8.7 (7)[c]
C(B)	0.090 (3)	0.5	0.325 (4)	11 (1)[c]
C(C)	0.040 (3)	0.5	0.697 (4)	11 (1)[c]

[a] Anisotropically refined atoms are given in the form of the isotropic equivalent thermal parameter defined as the following: $^4/_3[a^2\beta_{11} + b^2\beta_{22} + c^2\beta_{33} + ab(\cos\gamma)\beta_{12} + ac(\cos\beta)\beta_{13} + bc(\cos\alpha)\beta_{23}]$. [b] Estimated standard deviations in the least significant digits are given in parentheses. Values for which no esd's appear were not refined. [c] Refined isotropically.

Table V. Bond Distances (Å) and Angles (deg) for $Mo_2(\mu\text{-}SEt)_2Cl_4(dmpe)_2\cdot C_7H_8$ (**2**)

	Distances		
Mo–Mo′	2.712 (3)	S–C(1)	1.85 (2)
Mo–Cl	2.417 (3)	C(1)–C(2)	1.57 (3)
Mo–P	2.541 (3)	C(3)–C(3)‴	1.54 (3)
Mo–S	2.411 (4)	C(A)–C(B)	1.59 (3)
P–C(3)	1.870 (14)	C(A)–C(C)	1.85 (3)
P–C(4)	1.847 (14)	C(B)–C(C)′	1.68 (4)
P–C(5)	1.804 (13)		
	Angles		
Mo′–Mo–Cl	98.55 (8)	Mo–P–C(3)	108.1 (5)
Mo′–Mo–P	140.25 (9)	Mo–P–C(4)	117.65 (5)
Mo′–Mo–S	55.77 (6)	Mo–P–C(5)	119.2 (6)
Cl–Mo–Cl‴	162.9 (2)	C(3)–P–C(4)	104.5 (8)
Cl–Mo–P	85.2 (1)	C(3)–P–C(5)	101.6 (8)
Cl–Mo–P‴	81.7 (1)	C(4)–P–C(5)	103.7 (8)
Cl–Mo–S	91.6 (1)	Mo–S–Mo′	68.5 (1)
Cl–Mo–S′	98.0 (1)	Mo–S–C(1)	112.2 (5)
P–Mo–P‴	79.5 (2)	S–C(1)–C(2)	108 (1)
P–Mo–S	164.0 (1)	P–C(3)–C(3)‴	109.5 (9)
P–Mo–S′	84.5 (1)	C(B)–C(A)–C(C)	170 (3)
S–Mo–S′	111.5 (1)	C(A)–C(B)–C(C)′	92 (3)
		C(A)–C(C)–C(B)′	99 (2)

atoms were positioned in a mirror plane so that the symmetry of the toluene unit was 2/*m*. This necessitated a disordered location for the methyl carbon atom of the toluene molecule and, not surprisingly, this carbon atom could not be located in a difference map.

The three solvent atoms were refined isotropically, while all other atoms were refined anisotropically. After convergence of refinement, a difference map contained one peak more dense than 1.0 e/Å^3. This peak was less than 1.2 Å away from toluene carbon atom C(A), but an effort to refine it as the disordered methyl carbon atom resulted in unreasonable C–C distances and C–C–C angles. The final atomic positional and isotropic-equivalent thermal parameters are listed in Table IV. Anisotropic thermal parameters are available as supplementary material, and bond distances and angles are given in Table V.

Magnetic Measurements. Polycrystalline samples of the complexes were measured with a Model 905 superconducting SQUID susceptometer from S.H.E. Corp. operating at a measuring field of 5.00 kOe. Measurement and calibration techniques are reported elsewhere.[25] The sample holders were fabricated from an Al/Si alloy provided by the S. H. E. Corp., and the magnetism of the sample holder was checked over the entire measurement range (10–400 K). The magnetic data were corrected at each temperature for the magnetic contribution of the sample bucket. Table VII (supplementary material) lists the molar magnetic susceptibility data for each of the complexes corrected for the magnetic contribution of the sample bucket and for the diamagnetism of the constituent atoms using Pascal's constants. The magnetic data for the three complexes are plotted in Figures 10–12.

(25) O'Connor, C. J. *Prog. Inorg. Chem.* **1982**, *29*, 203 and references cited therein.

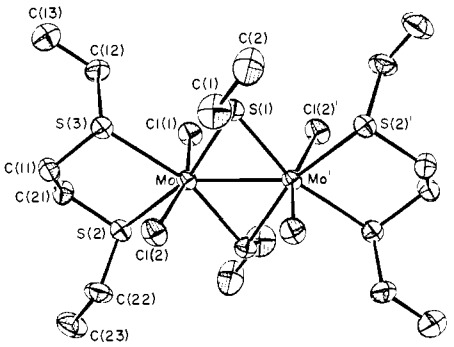

Figure 1. An ORTEP view of the structure of $Mo_2(\mu\text{-}SEt)_2Cl_4(dto)_2$ (**1**) with thermal ellipsoids drawn at the 50% probability level.

Results and Discussion

Preparative Reactions. Three procedures have been used to obtain compounds **1**–**6**. These are described by equations 1–3.

$$K_4Mo_2Cl_8 + 3EtSCH_2CH_2SEt \rightarrow Mo_2(\mu\text{-}SEt)_2Cl_4(dto)_2 + 4KCl + \text{“}C_2H_4\text{”} \quad (1)$$

$$Mo_2Cl_8^{4-} + 2dto + RSSR \rightarrow Mo_2(\mu\text{-}SR)_2Cl_4(dto)_2 + 4Cl^- \quad (2)$$

$$Mo_2Cl_4(LL)_2 + RSSR \rightarrow Mo_2(\mu\text{-}SR)_2Cl_4(LL)_2 \quad (3)$$

Reaction 1 is not general, nor does it give practical bulk yields even for compound **1**, which was first obtained by that method. It is of interest chiefly because of its novel character, but it does have one practical aspect: it generates compound **1** in crystalline form, albeit in only small quantities, and it was with crystals so obtained that the structure of **1** was determined. The EtS groups evidently arise from the dto employed and at least formally C_2H_4 must also be produced, but we have not detected it, either as such or in the form of any other product from the fragmentation of the dto.

The procedure represented by reaction 1 is reproducible, but it always gives a low yield of **1** since most of the starting materials remain unreacted. A similar reaction mixture was previously used[4] to make $Mo_2Cl_4(dto)_2$ and none of **1**, but the different result appears to be due to the use of different sources of the $Mo_2Cl_8^{4-}$ ion. Previously,[4] $(NH_4)_5Mo_2Cl_9\cdot H_2O$ was used and its greater solubility allowed $Mo_2Cl_4(dto)_2$ to form and precipitate rapidly. A small amount of HCl was added to increase the solubility of $(NH_4)_5Mo_2Cl_9\cdot H_2O$ and catalyze the reaction. Although not described in detail in the Experimental Section, reaction 1 has been repeated except that HCl was added and the mixture was stirred at 45 °C for 6 h. $Mo_2Cl_4(dto)_2$ was produced in 69% yield.

Compound **1** is produced in better yield (up to 49%) with use of reaction 2. Compound **4** may also be prepared in this manner. Both **1** and **4** are most likely produced by the initial formation of $Mo_2Cl_4(dto)_2$ followed by oxidative addition of RSSR. This pathway is supported by the fact that if $Mo_2Cl_8^{4-}$ and EtSSEt are refluxed together before adding dto, then a compound **1a** with an IR spectrum quite different than that of **1** is formed. The fact that the yields obtained with reaction 2 are still rather low is most likely because a side reaction occurs even when dto and RSSR are added simultaneously, as evidenced by the isolation of **1a** and **4a**.

The above explanation for the course of events in reaction 2 is further supported by the fact that compounds **1**, **2**, **3**, **4**, **5**, and **6** can each be prepared with use of reaction 3. The reactions of β-$Mo_2Cl_4(dmpe)_2$ with EtSSEt to yield **2** and with PhSSPh to yield **5** are particularly noteworthy since the dmpe ligands are bridging in the starting material and chelating in the products. Interestingly, reaction 3 fails to occur in the cases of $Mo_2Cl_4(dppm)_2$ + PhSSPh and $Mo_2Cl_4L_4$ + EtSSEt (L = PMe_3 or PMe_2Ph).

Structures. The compounds that form the subject of this investigation do not easily form crystals suitable for single-crystal X-ray structural study. Crystallographic studies have therefore been limited to two of them, but there is no reason to doubt that

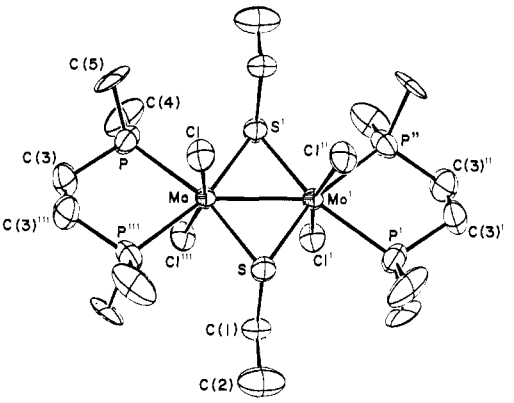

Figure 2. An ORTEP view of the $Mo_2(\mu\text{-}SEt)_2Cl_4(dmpe)_2$ molecule in compound **2**. Thermal ellipsoids enclose 50% of the electron density. Singly primed, doubly primed, and triply primed atoms are related to unprimed atoms by an inversion center, mirror plane, and a twofold axis, respectively.

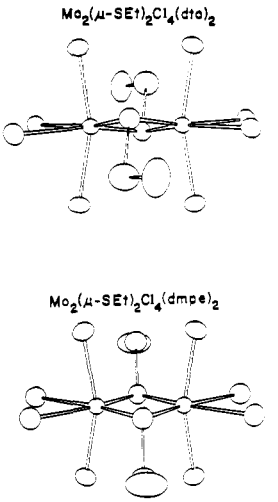

Figure 3. Comparison of the central portions of compounds **1** and **2**.

these two, which have very similar structures, are representative.

Compound **1**, $Mo_2(\mu\text{-}SEt)_2Cl_4(dto)_2$, consists of molecules whose structure is shown in Figure 1. There is a crystallographic center of inversion midway between the metal atoms, and the overall approximate symmetry of the molecule is not any greater than this owing to the orientations of the ethyl groups of the bridging EtS groups, namely, one up and one down relative to the central $S_2MoS_2MoS_2$ plane. Considering only the metal atoms and those coordinated to them, i.e., the $Mo_2(\mu\text{-}S)_2S_4Cl_4$ set, the symmetry can be idealized to D_{2h}. The bridge bonding is essentially symmetrical, with Mo–S = 2.403 (1) Å and Mo′–S = 2.400 (1) Å. The other various sets of distances and angles that are crystallographically independent but ought to be equal under D_{2h} symmetry are equal within the experimental uncertainties. Thus, the Mo–Cl distances are 2.402 (1) and 2.403 (1) Å and the terminal Mo–S distances are both 2.579 (1) Å. It is to be noted that the Mo–S(br) distances are considerably shorter than the Mo–S(t) distances, the Mo–S(br)–Mo angles are very small (averaging 56.06°), and the Mo–Mo distance is 2.682 (1) Å. The structure thus clearly implies that there is appreciable direct Mo–Mo bonding. We shall discuss this in a later section.

The structure of the dimolybdenum molecule in compound **2**, $Mo_2(\mu\text{-}SEt)_2Cl_4(dmpe)_2\cdot C_7H_8$, is illustrated in Figure 2. Its overall similarity to that of $Mo_2(\mu\text{-}SEt)_2Cl_4(dto)_2$ is obvious. This edge-sharing bioctahedron has crystallographic $2/m$ (C_{2h}) symmetry; the twofold axis is coincident with the Mo–Mo line, and the mirror plane contains the six atoms of the two μ-SEt groups. There is, of course, also a center of inversion midway between the two Mo atoms. Once again, the central group of atoms consisting of the two metal atoms and the ten atoms directly bonded to them conform very closely to the dictates of D_{2h} symmetry. There is clear evidence of pronounced bonding between the molybdenum atoms, although it is slightly weaker with the Mo–Mo distance being 2.712 (3) Å.

The one notable dissimilarity between the structures of **1** and **2** is to be found in the Mo–S–C–C torsion angles, which differ by more than 30°. This is made clear in Figure 3. This difference may be understood by considering the different steric demands made upon the μ-SEt ligands by the dto and dmpe ligands. In the case of the dmpe complex, there are eight methyl groups, four above and four below the central plane. There is nothing to be gained sterically for the ethyl groups of the μ-SEt groups to be directed toward either end of the molecule, and they therefore remain strictly in the central plane. In the case of the dto molecule, however, there are two ethyl groups on each end, two up and two down. The ethyl groups of the μ-SEt ligands, each on the opposite side of the central plane from the two dto ethyl groups on its own side of the molecule, are free to turn out of the central region, and they do so.

The structural relationships between starting materials and products in these oxidative addition reactions, which are summarized in Figure 4, are of interest. The top reaction[4] is known in only one case and is not likely to be of general importance since even in that case the yields are small. The stereochemistry of the product may be possible only when the bridging groups are monatomic; when μ-SEt groups are present together with the ethyl groups of dto ligands there would be steric inference tending to favor the type of structure we have found in the present study. The fact that both α (chelated) and β (bridged) isomers of $Mo_2Cl_4(LL)_2$ compounds react, as shown, to form the same type of product may seem surprising (especially the ready reactivity of the β-type reactant), but it is in keeping with the known interconvertability of such α and β isomers.[13] The lack of reactivity of both $Mo_2Cl_4(dppm)_2$ and $Mo_2Cl_4(PMe_3)_4$ does not have any obvious explanation in terms of the stereochemistry of the products. The type of dppm-bridged molecule shown in Figure 4 is known in several cases, including $Mo_2Cl_6(dppm)_2$.[14] While the replacement of μ-Cl groups by μ-SEt groups might introduce some steric strain, it is not evident that it should render such a product altogether inaccessible. Nor would a molecule of the type $Mo_2(\mu\text{-}SR)_2\text{-}Cl_4(PMe_3)_4$ appear to be sterically unacceptable in view of the known existence of $Ta_2Cl_6(PEt_3)_4$ recently described

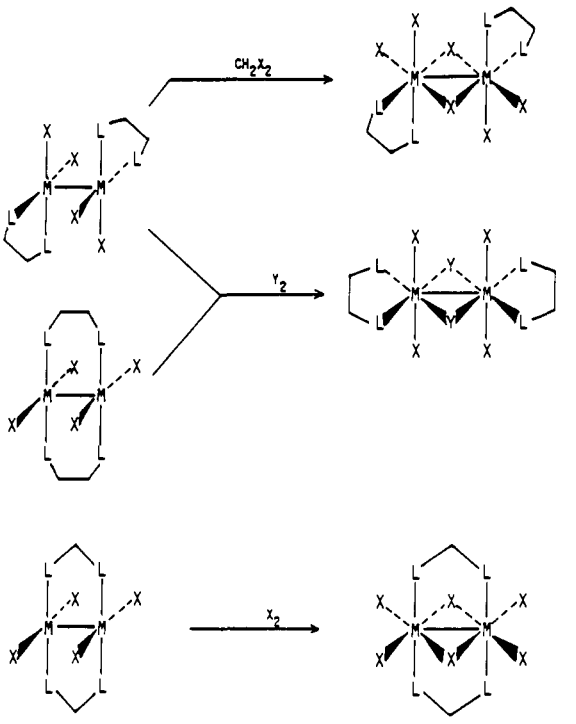

Figure 4. Three possible isomers (A, B, C) of an $Mo_2(\mu\text{-}X)_2X_4(LL)_2$ complex and oxidative addition reactions which lead to them.

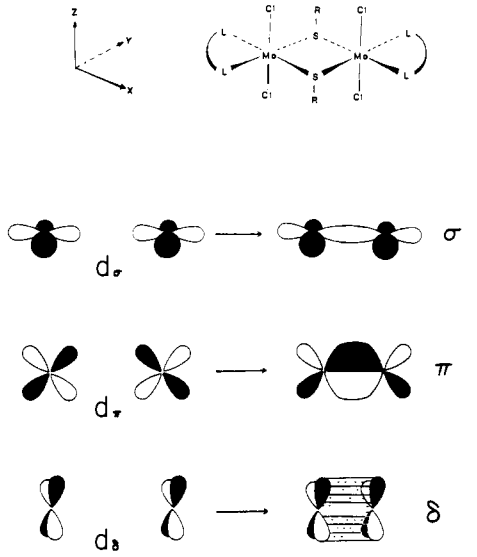

Figure 5. Illustration of metal–metal bonding possibilities based on metal d orbitals alone.

by Sattelberger, Wilson, and Huffman.[15]

Metal–Metal Bonding. A major reason for interest in molecules of the type under discussion here is the question of how the d^n configurations (d^3 in the present instances) on the two metal atoms will interact with each other to give rise to direct metal–metal bonding. A kind of zeroth order view of the problem is provided by simply noting that within each of the two (in these cases, equivalent) local octahedra there are three d orbitals that are not of suitable lobal structure to participate in metal–ligand σ bonding.[16] These three orbitals may legitimately be chosen (i.e., in a manner consistent with the overall D_{2h} symmetry of the M_2X_{10} skeleton) to be as shown in Figure 5, and thus the formation of one σ bond, one π bond, and one δ bond may be envisioned.

As already pointed out by Shaik, Hoffmann, Fisel, and Summerville,[17] the fact that the ligands, especially the two bridging ligands, have orbitals that interact with these idealized metal orbitals makes the situation somewhat more subtle. It means, in fact, that a reliable analysis of the metal–metal bonding possibilities requires at least an approximate computational treatment of the molecule as a whole rather than just a consideration of the metal orbitals alone. Hoffmann and co-workers chose the extended Hückel approximation for their work and chose Re_2Cl_{10} as their representative system.

In this laboratory we often[18,19] employ the Fenske–Hall method[20] to provide approximate descriptions of molecular electronic structures and continue to do so here. Figure 6 shows the results for the Mo_2Cl_{10} molecule. It is encouraging to see that there is a good general similarity to the results of Hoffmann et al. for Re_2Cl_{10}, including the counterintuitive features that at longer distances (including the actual distance) the σ^* orbital lies lowest and the δ^* orbital lies lower than the δ orbital. As in the case of Re_2Cl_{10}, it is clear that no metal–metal bond is present. We have previously examined a W(IV)–W(IV) case in which a W=W bond is present.[21]

We turn now to the cases of direct interest, namely the d^3–d^3 systems with SR bridges. In our calculation we have modeled this type of system with $Mo_2Cl_4(\mu\text{-}SH)_2(SH_2)_4$. The results of the Fenske–Hall calculation are shown in Figure 7. The pattern here is somewhat more in accord with intuitive expectation, in the sense that the σ and σ^* levels are always lowest and highest, respectively, and next lowest and next highest levels are always π and π^*, respectively. Once again, however, there is a region where the δ^* level is more stable than the δ level.

We were sufficiently concerned to assess the level pattern reliably that we also carried out an SCF–Xα–SW calculation on the same model system, but only at the observed Mo–Mo distance for **1**, viz., 2.68 Å. A comparison of these results with those from the Fenske–Hall calculation is shown in Figure 8. It is evident

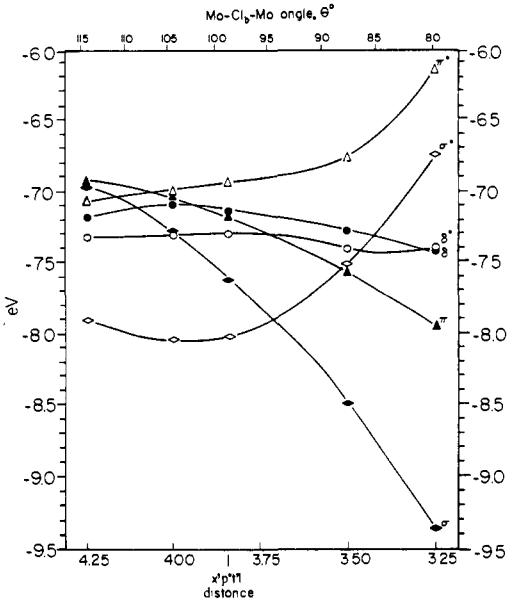

Figure 6. The behavior of the metal-based σ, π, δ, δ^*, π^*, and σ^* orbitals as given by a Fenske–Hall calculation over a range of Mo–Mo distances for Mo_2Cl_{10}.

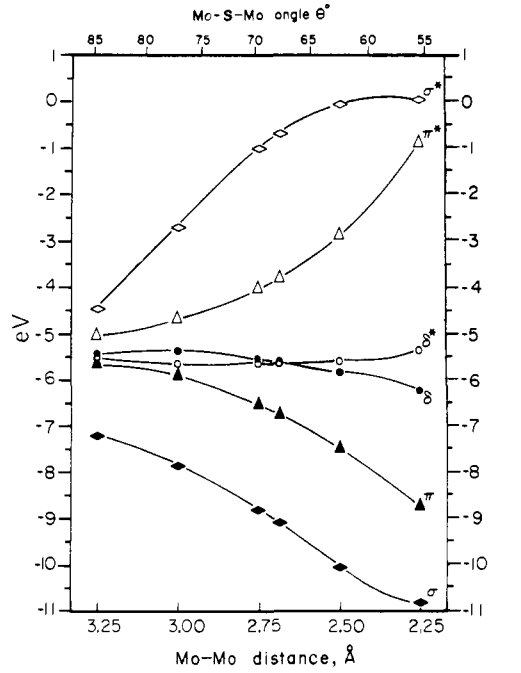

Figure 7. The results of Fenske–Hall calculations on a $Mo_2Cl_4(\mu\text{-}SH)_2(SH_2)_4$ molecule for a range of Mo–Mo distances.

that the Fenske–Hall calculation gives much larger energy differences, but the pattern is very similar. This feature of Fenske–Hall results is not unusual. The behavior of the δ and δ^* levels is of particular interest. The SCF–Xα–SW calculation also places these two levels extremely close together, although it inverts the order. We do not believe that either calculation can be trusted to provide the correct ordering of two levels that are so close together, and therefore we would not venture to say which one we think is right in this case.

The feature to which we now direct attention is the fact that, regardless of the exact ordering, the δ and δ^* levels have very similar energies. The principal consequences of this for a d^3–d^3 system of the sort we are dealing with are both structural and magnetic. Structurally, the effective Mo–Mo bond order will be two, based on the fact that the bonding σ and π levels are each doubly occupied; the δ and δ^* levels are both virtually nonbonding. The conclusion that the Mo–Mo bond order is essentially two is

Table VI. Parameters from the Best Fit to Equation 1 to the Magnetic Data for Three Binuclear Molybdenum Compounds

complex	g	$E(^3B_{1u})$ (cm^{-1})	$E(^1B_{1u})$ (cm^{-1})	$E(^1A_{1g}^*)$ (cm^{-1})	TIP (emu/mol)	% impurity
1	2.00	680	965	1930	0.000226	0.18
2	2.00	1077	2200	4400	0.000650	2.10
4	2.00	807	1095	2190	0.000590	0.26

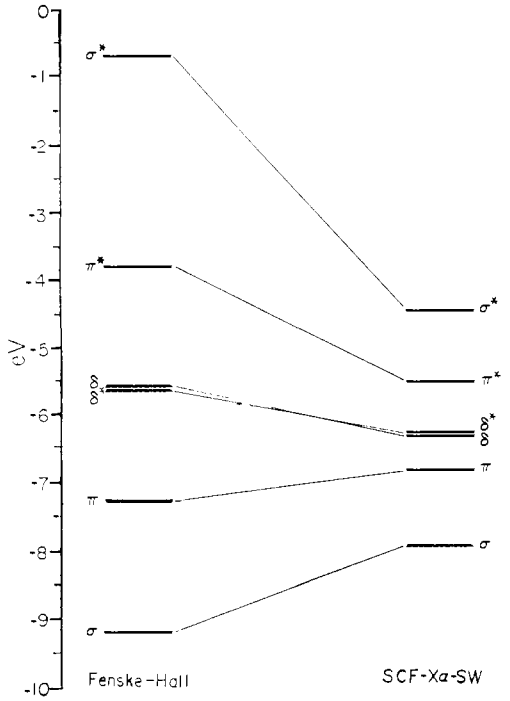

Figure 8. A comparison of the results of the Fenske–Hall calculation and an SCF–Xα–SW calculation on $Mo_2Cl_4(\mu\text{-}SH)_2(SH_2)_4$, both done at the Mo–Mo distance of 2.68 Å.

consistent with the observation of Mo–Mo distances of about 2.70 Å. In a number of edge-sharing bioctahedral systems where only four electrons are available for metal–metal bonding and the bridging groups are either Cl^- or RS^-, the M≡M bond lengths are all in the range 2.69–2.76 Å. The relevant examples, with their M≡M distances in angstroms, are as follows:

$Ta_2Cl_6(PMe_3)_4$ 2.721 (1)[21]

$Nb_2Cl_6(dppm)_2$ 2.691 (1)[22]

$Nb_2Cl_6(dppe)_2$ 2.721 (2)[23]

$W_2Cl_6(\mu\text{-}SPh)_2(SMe_2)_2$ 2.759 (1)[24]

Magnetic Behavior. The magnetic behavior of these molecules will be determined by the electronic states that are thermally accessible. Because of the very similar energies of the δ and δ^* orbitals, several states must be considered. Although the relative energies of the δ and δ^* orbitals are uncertain, the qualitative pattern of states to be considered is predictable. In Figure 9 we show what is expected for $E(\delta) < E(\delta^*)$. A little reflection will show that the pattern of states to be expected in the case that $E(\delta^*) < E(\delta)$ is the same, viz., the lowest and highest states will be $^1A_{1g}$ and in between there are $^3B_{1u}$ and $^1B_{1u}$ states, in the order shown arising from the $\delta\delta^*$ configuration.

The magnetic susceptibility for a molecule that has energy levels corresponding to the diagram shown in Figure 9 may be derived following the van Vleck formula[25] and is given by the following closed form equation where $X_1 = E(^3B_{1u})/kT$, $X_2 = E(^1B_{1u})/kT$,

$$\chi = \frac{Ng^2\mu_B^2}{kT}\,\frac{2e^{-x_1}}{1 + 3e^{-x_1} + e^{-x_2} + e^{-x_3}} \qquad (I)$$

and $X_3 = E(^1A_{1g}^*)/kT$ and the energy terms refer to the energy level diagram in Figure 9. Magnetic susceptibility data for

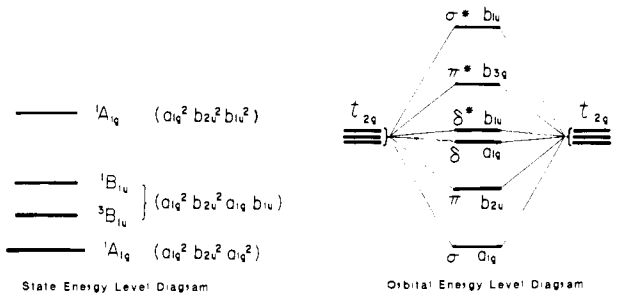

Figure 9. Qualitative orbital and state energy level diagrams for the case where $E(\delta) < E(\delta^*)$.

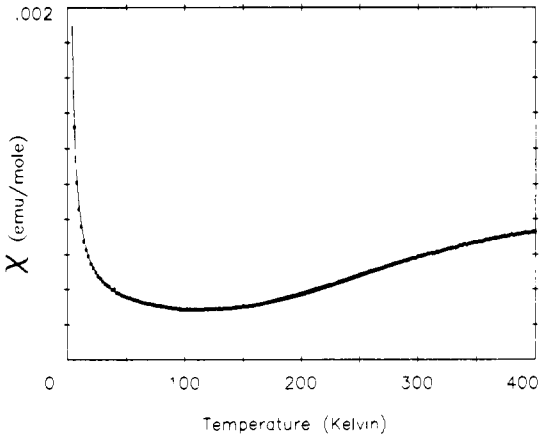

Figure 10. A plot of corrected molar magnetic susceptibility vs. temperature for compound **1**. Points are experimental and the line is from eq 1 with the parameters listed in Table VI.

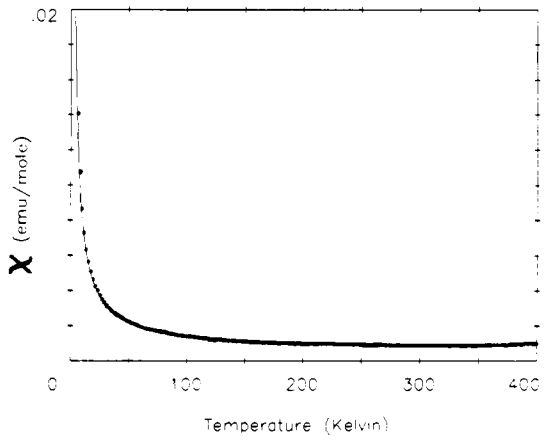

Figure 11. A plot of corrected molar magnetic susceptibility vs. temperature for compound **2**. Points are exerimental and the line is from eq 1 with the parameters listed in Table VI.

compounds **1**, **2**, and **4** are shown in Figures 10, 11, and 12. The solid lines show how these data were fitted with eq 1, including corrections for temperature-independent paramagnetism and a paramagnetic impurity assumed to be a Mo(III) monomer with $S = {}^3/_2$. The quality of the fit was very sensitive to the value of $E(^3B_{1u})$, but the magnitudes of the singlet energy levels had a substantially smaller effect on the shape of the susceptibility curve. A wide range of values, including complete omission of one of these terms, gave acceptable fits. In view of this lack of sensitivity, the

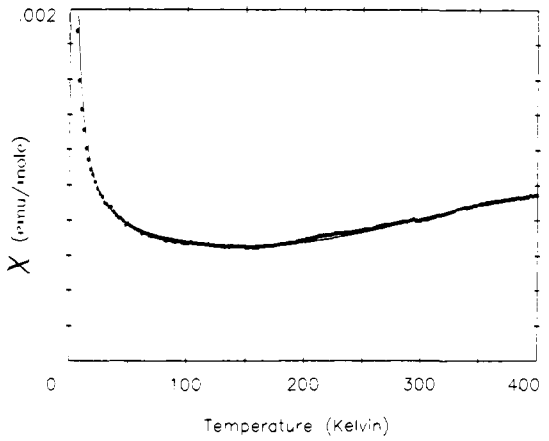

Figure 12. A plot of corrected molar magnetic susceptibility vs. temperature for compound **4**. Points are experimental and the line is from eq 1 with the parameters listed in Table VI.

energies of the singlet states were constrained so that the energy of the $^1A_{1g}$* state is always twice that of the $^1B_{1u}$ state, which should, of course, be approximately true. The fitted parameters for **1**, **2**, and **4** are listed in Table VI.

In assessing the significance of the parameters in Table VI, several points should be noted. First, as already mentioned, the energies of the excited singlet states were artifically coupled in the fitting process. Second, it was assumed that there are no individual high-frequency terms in the van Vleck derivation associated with each of the excited states, even though the ground state has a detectable temperature-independent paramagnetism. Instead, a single high-frequency term (TIP) was uniformly applied over the entire temperature region without a Boltzmann weighting parameter. To incorporate and allow free variation for all of the possible terms would result in a meaningless overparameterization; however, their omission requires that the parameters that are obtained be viewed with the proper caution. This is especially true for the fitted energies of the two singlet states, since they are least effective in modifying the shape of the fitted curve and are thus subject to large uncertainties in the fitting process. Nevertheless, the inclusion of the singlet terms did improve the quality of the fit noticeably. The energy of the paramagnetic $^3B_{1u}$ state is quite accurate since this term is by far the dominant one in determining the shape of the magnetic susceptibility curve.

The application of molecular orbital theory to these simple binuclear molecules provides a consistent explanation for the unusual magnetic phenomena exhibited by these molecules. Their magnetic properties cannot be explained adequately by a spin $^3/_2$ dimer formulation because the energy level diagram for spin $S = {}^3/_2$ has a larger number of magnetic multiplets and the shape of the χ vs. T curve is quite different.

Concluding Remarks

Although many dinuclear systems with multiple metal–metal bonds have been prepared and characterized, only recently has the spin triplet state of the $\delta\delta^*$ configuration been observed. This is true despite the theoretical[26,27] and indirect experimental evidence[27,28] which predicts that the $^3(\delta^*\delta)$ configuration is the lowest excited state in those metal-bonded systems that exhibit δ bonds.

An attempt to characterize magnetically the excited antibonding states occurred several years ago when Pasynskii and co-workers[29] invoked molecular orbital theory to explain the antiferromagnetic exchange in some binuclear chromium(III) complexes. However, their theoretical analysis incorporated the Heisenberg–Dirac–Van Vleck Hamiltonian for a spin $S = {}^3/_2$ coupled dimer and the magnetic properties were successfully explained by using the magnetic exchange model. However, intricacies of the metal–metal bonding energy levels were not manifested in these complexes, and the nature of the electronic interactions therefore remained in doubt. In our initial communication[2] describing the synthesis of these complexes, we gave a preliminary report of the first direct magnetic detection of a $^3(\delta\delta^*)$ state that could only be reasonably accounted for by the excited triplet that arises as a result of the metal orbital bonding overlap. More recently Hopkins, Gray, and co-workers[30] have also reported the magnetic observation of the excited spin triplet configuration for $Mo_2Cl_4(dmpe)_2$, a binuclear with a quadruply-bonded ground state.

Acknowledgment. We thank the National Science Foundation for support. We are grateful to Professor B. Hutchinson of Abilene Christian University for some preliminary magnetic measurements.

Registry No. 1, 90029-94-0; **2**, 90029-97-3; **3**, 98777-06-1; **4**, 90029-95-1; **5**, 98777-07-2; **6**, 98854-89-8; $K_4Mo_2Cl_8$, 25448-39-9; $Mo_2Cl_4(dto)_2$, 67598-73-6; $Mo_2Cl_4(dmpe)_2$, 85115-86-2; $Mo_2Cl_4(dtd)_2$, 51731-35-2; $Mo_2Cl_4(dppm)_2$, 64490-77-3; $Mo_2Cl_4(PMe_3)_4$, 67619-17-4; $Mo_2Cl_4(PMe_2Ph)_4$, 38832-73-4; $Mo_2Cl_4(\mu\text{-}SH)_2(SH_2)_4$, 98799-12-3; $(NH_4)_5Mo_2Cl_9$, 61583-95-7; EtSSEt, 110-81-6; Mo, 7439-98-7.

Supplementary Material Available: Tables of anisotropic thermal vibration parameters and structure factors for **1** and **2** and numerical magnetic susceptibility data for **1**, **2**, and **4** (25 pages). Ordering information is given on any current masthead.

(26) Hay, P. J.; Thibeault, J. C.; Hoffmann, R. *J. Am. Chem. Soc.* **1975**, *97*, 4884. Hansen, A. E.; Ballheusen, C. J. *Trans. Faraday Soc.* **1965**, *61*, 631.

(27) Miskowski, V. M.; Goldbeck, R. A.; Klijer, D. S.; Gray, H. B. *Inorg. Chem.* **1979**, *18*, 86.

(28) Zietlow, T. C.; Hopkins, M. D.; Gray, H. B. *J. Solid State Chem.* **1985**, *57*, 112. Hay, P. J. *J. Am. Chem. Soc.* **1982**, *104*, 7007.

(29) Pasynskii, A. A.; Eremenko, T. L.; Orazsokhatov, B.; Rakitin, Ya. V.; Novotortsev, V. M.; Ellert, O. G.; Kalinnikov, V. T.; *Inorg. Chim. Acta* **1980**, *39*, 91.

(30) Hopkins, M. D.; Zietlow, T. C.; Miskowski, V. M.; Gray, H. B. *J. Am. Chem. Soc.* **1985**, *107*, 510.